Journal of Himalayan Earth Sciences Volume 59, No. 1, 2026 pp. 118-141

Hydrological Response and Flood Potential Assessment of a Tropical Small Island: Integration of Geomorphometric Indices and Water Balance in Wai Ruhu Watershed, Ambon, Maluku, East Indonesia

Nabila Kalsum Tuanany[1*], Emi Sukiyah[2], Boy Yoseph CSSSA[2], and Axl Manuhutu[3]

[1] Master Program of Geological Engineering, Universitas Padjadjaran, Bandung 40132, Indonesia

[2] Faculty of Geological Engineering, Universitas Padjadjaran, Sumedang 45363, Indonesia

[3] Master's Program of School of Minerals and Energy Resources Engineering, University of New South Wales (UNSW), Australia

**Corresponding Author: nabila17024@mail.unpad.ac.id*

Submitted Date:13/01/2026 Acceptance Date: 01/03/2026 Publication Date: 31/03/2026

Abstract

High annual rainfall on Ambon Island significantly increases its vulnerability to hydrological disasters, particularly flooding. This study evaluates flood potential in the Wai Ruhu Watershed by integrating geomorphometric indices with water balance analysis. Geomorphological characteristics, including stream order, bifurcation ratio (Rb), drainage density (Dd), form factor (Rf), circularity ratio (Rc), and elongation ratio (Re), were analyzed using ArcGIS 10.8. The water balance was determined using 11 years of precipitation and evapotranspiration data (2014–2024), while surface runoff and infiltration were estimated based on land cover and slope gradients. The results indicate that the watershed's low bifurcation ratio and moderate-high drainage density reflect a rapid hydrological response and strong structural control on flow. Furthermore, steep topography and land cover changes significantly increase the runoff coefficient, leading to high surface discharge and limited infiltration. The integration of these parameters confirms a high flood risk, particularly in densely populated downstream areas. These findings provide a critical framework for watershed management and land-use planning to mitigate hydrological hazards in small tropical island environments such as Ambon City.

Keywords: Geomorphometric indices; water balance; flood potential, small tropical islands; Wai Ruhu Watershed

1. Introduction

A watershed is a land area that collects and stores rainwater, which subsequently drains into a lake or through a river system (Obeidat et al., 2021). Morphometric analysis is a crucial aspect of watershed management, as it provides a quantitative description of drainage system characteristics, including dimensions and geometry (Mohammed et al., 2018; Strahler, 1964).

In addition to physical characteristics, the functional behavior of a watershed can be understood through the concept of water balance, which describes the relationship between total water inflow and total water outflow (Duque et al., 2025; Rahmanda and Dasanto, 2018). This analysis estimates water volume using inflow parameters such as rainfall, groundwater, and surface runoff, and outflow parameters such as evaporation and groundwater discharge (Suhernomo et al., 2023). Imbalances in these components can directly trigger hydrological hazards such as floods and droughts (Trifonova et al., 2016), as all water within the catchment ultimately flows toward the outlet regardless of its pathway (Sambodo et al., 2025).

Based on data from the Pattimura Meteorological Station (2014–2024), the average annual rainfall on Ambon Island reaches 3,607.6 mm/year, which is classified as very high. These extreme climatic conditions make Ambon Island one of the regions with the highest rainfall intensity in Indonesia and significantly increase the risk of flash floods (Bashir and Alsalman, 2024; Sinay et al., 2020). This recurring flood phenomenon indicates a decline in watershed quality in the region (Tutuarima et al., 2021). While several triggering factors, such as short-duration extreme rainfall producing high-velocity runoff, have been identified (Şen et al., 2013; Abdalla et al., 2014; Elkhrachy, 2015; Alarifi et al., 2022), comprehensive studies integrating geological, geomorphological, and land-cover characteristics of the Wai Ruhu Watershed remain limited. The watershed, which is the largest in southern Ambon with an area of 15 km² (Tuanany et al., 2024), requires further investigation to quantify the extent to which physical degradation contributes to flood vulnerability.

The integration of morphometric analysis and water balance is essential for a comprehensive understanding of watershed hydrological response. Morphometric parameters such as stream order, bifurcation ratio (Rb), drainage density (Dd), elongation ratio (Re), circularity ratio (Rc), and form factor (Rf) provide insights into the surface flow system and river discharge formation (Sukiyah et al., 2015; Gentana et al., 2018; Haryanto et al., 2019; Folharini et al., 2022). In contrast, hydrological components, including precipitation, evapotranspiration, infiltration, and runoff, represent dynamic water volume processes. Integrating these approaches enables a more accurate estimation of hydrological contributions and improves flood hazard prediction (Rendra, 2023; Rendra and Sukiyah, 2021).

This study aims to analyze the relationship between morphometric characteristics and water balance conditions in the Wai Ruhu Watershed to improve flood risk assessment. The novelty of this research lies in integrating quantitative morphometric parameters with recent decadal hydrological data in a small island watershed characterized by extremely high rainfall. This manuscript is structured systematically, beginning with the analysis of morphometric characteristics, followed by water balance calculations, integrated interpretation of hydrological responses, and concluding with recommendations for disaster risk management.

2. Study Area and Geological Setting

Administratively, the Wai Ruhu watershed is located in Sirimau District, Ambon City, Maluku Province, Indonesia. Geographically, this area is located at 128°05”22’ E–128°14”35’ E and 3°47”31’ S – 3°40”50’ S. The detailed location of the study can be seen in Fig. 2.

Since the late Oligocene, Eastern Indonesia has been the convergence zone of three major tectonic plates, namely the Eurasian, Pacific, and Indo-Australian plates (Hall, 2012; Pownall et al., 2013; Watkinson et al., 2021). The interaction between these three plates forms a subduction zone in the form of a trench with a depth ranging from 4,500 to 7,000 meters (Supartoyo and Putranto, 2014) and produces a tectonic arc system known as the Banda Arc (Bakker et al., 2023). According to Spakman and Hall (2010), the Banda Arc is divided into two main parts, namely the outer arc (non-volcanic), composed of sedimentary, metamorphic, and some igneous rocks dating from the Permian to Quaternary periods, and the inner arc (volcanic), which has been active since the Late Miocene (Honthaas et al., 1998; Lewerissa et al., 2017). Geologically, Ambon Island is located above the inner arc and is part of the Maluku Orogen (Hermawan and Yushantari, 2010). Located south of Seram Island and bordering the Banda Sea, this position places Ambon Island in the Australian-Asian transition zone, which is part of the Eurasian plate (Bemmelen, 1949).

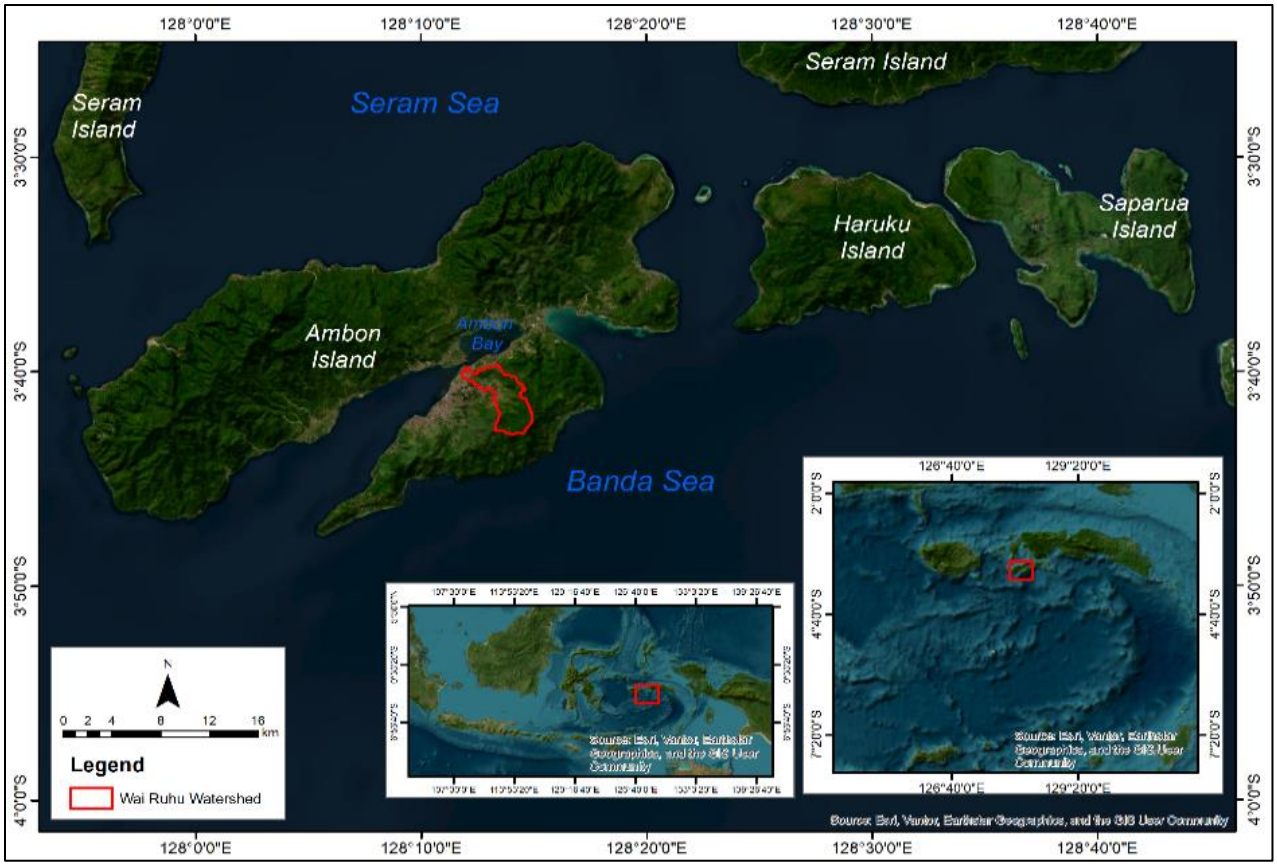

Fig. 1. Location of the Wai Ruhu Watershed is marked in Red on the Map.

The physiography of Ambon Island can be divided into four physiographic units namely the volcanic unit that dominates the highlands, characterized by dendritic and sub-parallel flow patterns; intermountain depressions that form plateaus on the ridges, which are also associated with uplifted coral reef terraces and marked by the presence of several sinkholes in the flow patterns, raised coral reef terraces, and alluvial plains that extend along the coast (Wattimena and Handoko, 2016).

Geologically, the Wai Ruhu watershed from upstream to downstream is composed of several types of lithology, including: Jurassic-Cretaceous ultramafic rocks (JKu); a small distribution of Late Triassic- Jurassic Kanikeh Formation (Trjk) in the upstream section; Ambon volcanic rocks (Tpav) or Ammonite dating from the Pliocene; and Coral Limestone (Qi) and Alluvium (Qa) dating from the Quaternary (Tjokrosapoetro et al., 1993). A regional geological map modified by the author for this area can be seen in Fig. 3.

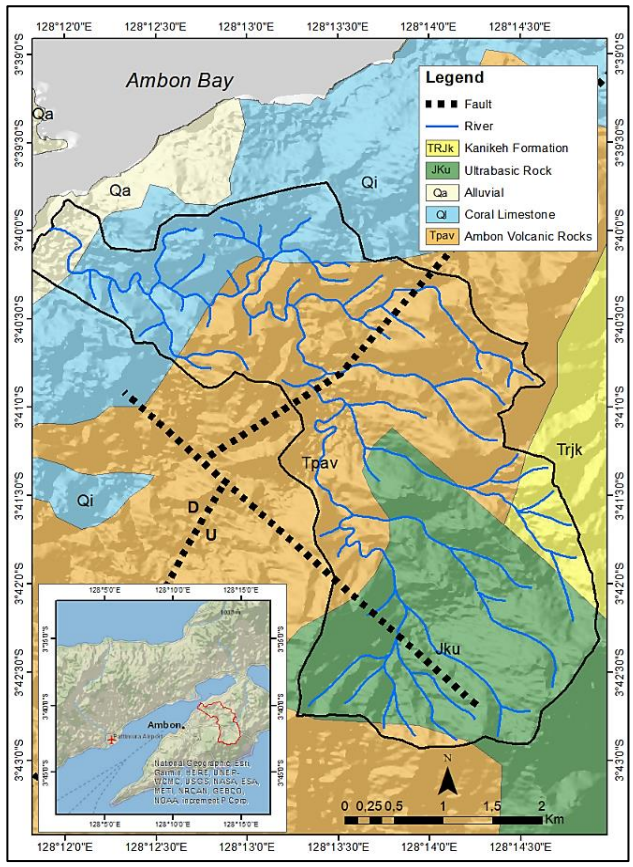

Fig. 2. Regional Geological Map modified after Tjokrosapoetro et al. (1993).

3. Materials and Methods

This study focuses on the Wai Ruhu watershed, where ArcGIS 10.8 software and statistics are used to analyze the integration of morphometric and hydrological dynamics. Geographic Information System (GIS) data can be used to identify affected areas and flood-prone areas, one of which is through morphometric index analysis (Sy et al., 2019; Ali et al., 2020; Ariyani et al., 2024). With the integration of geospatial techniques (GIS and RS) and mathematical modeling, morphometric parameters can be accurately measured and calculated to produce comprehensive regional characteristic data (Prasannakumar et al., 2013; Jaya et al., 2024). As shown in Fig. 1, the overall workflow includes key processes such as spatial data pre-processing, morphometric parameter extraction, and water balance estimation. This includes river network delineation, statistical validation through the Kruskal-Wallis test, and rainfall consistency using the RAPS (Rescaled Cumulative Deviations) method. All of these processes are integrated to provide a comprehensive assessment of flood potential in the Wai Ruhu watershed.

3.1 Watershed Morphometric Analysis

This study examines the analysis of morphometric characteristics and water balance in the Wai Ruhu watershed. The data used in this morphometric analysis are National Digital Elevation Model (DEM) data with a spatial resolution of 8 meters. ArcGIS 10.8 GIS software was employed for data processing. The morphometric parameters analyzed are as follows:

3.1.1 Stream Order

Stream order in a watershed can be divided into several river orders. River order refers to the position of the river channel branching relative to the main river within a watershed. As the river order increases, the total area and total length of the watershed will also increase. Based on the method of Strahler (1964) and Sukiyah (2017), a river that has no branches (in the upper reaches) is called a first-order river. The confluence of two first-order rivers is called a second-order river, and the confluence of two second-order rivers is called a third-order river, and so on downstream.

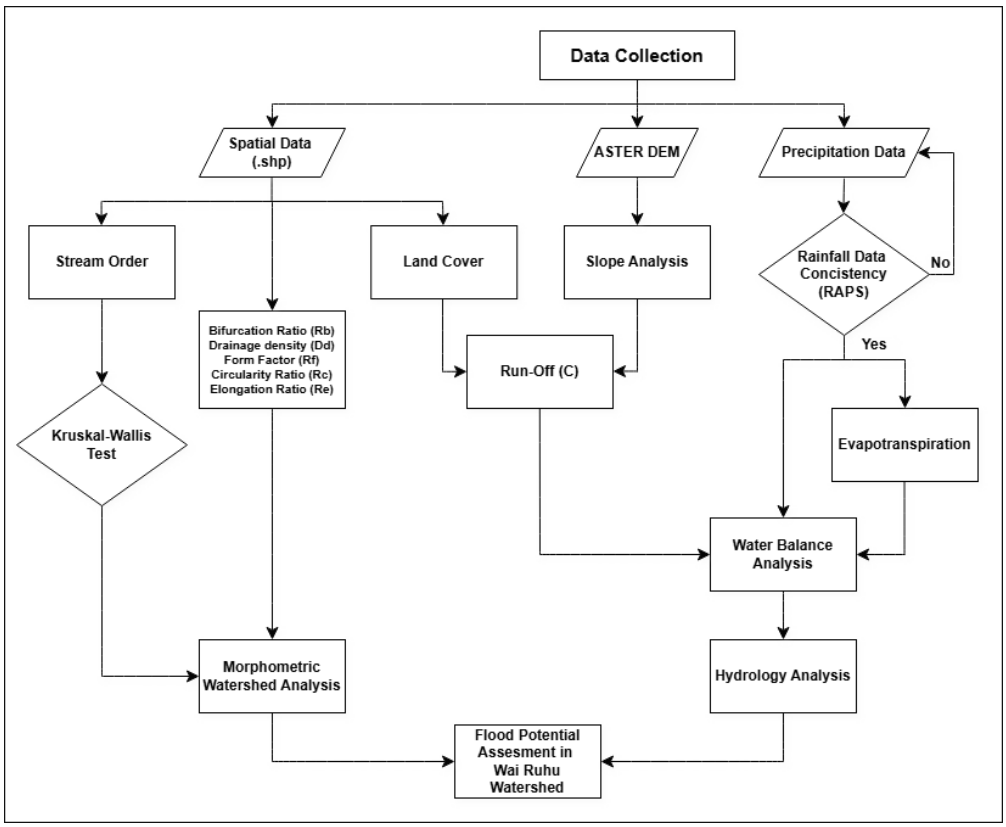

Fig. 3. Methodological flowchart of the study in Wai Ruhu Watershed.

3.1.2 Ratio of Bifrucation (Rb)

The bifurcation ratio (Rb) is defined as the ratio of the number of stream segments of a given order u by the number of stream segments of the next higher order (Schumm, 1956) in Dimple et al. (2022). The Rb calculation is performed using Equation (1):

$$Rb = \frac{(Nu)}{(Nu+1)} \quad \ldots\ldots\ldots (1)$$

Where, Rb = Bifurcation ratio index, Nu = Number of stream segments of order u, Nu + 1= Number of stream segments of the next higher order.

The classification of the bifurcation ratio (Rb) reflects the hydrological response and the influence of geological structure on a watershed. According to Soewarno (1991), an Rb value of less than 3 indicates a very rapid rise in flood water levels with a rapid decline, an Rb value of 3-5 indicates a not-too-rapid rise in flood water levels with a moderate decline, and an Rb value of more than 5 indicates a rapid rise in flood water levels with a slow decline. Meanwhile, according to Strahler (1964) in Verstappen (1983), an Rb value of less than 3 indicates slight tectonic deformation and a flow pattern that is not altered by the structure, an Rb value of 3-5 indicates no influence of tectonic deformation, and an Rb value of more than 5 indicates tectonic deformation. Meanwhile, an Rb value greater than 5 reflects a rapid rise in floodwater levels with a slow decline.

3.1.3 Drainage density (Dd)

Drainage density is the value of river length relative to catchment area (Horton, 1945). The drainage density value of a watershed is usually influenced by various factors such as the weathering resistance of the bedrock, the permeability of the overlying rock, climate, and vegetation (Javed et al., 2009). A low drainage density value indicates that the area has rocks with high permeability and coarse drainage texture, while a high value indicates the opposite (Van Zuidam, 1985; Sukiyah, 2017). Drainage density can also be used to indicate the hardness of rocks. Rocks with low Dd values tend to be harder than rocks with high Dd values (Sukiyah, 2012). Dd is calculated using Equation (2):

$$Dd = \frac{\Sigma L}{A} \quad \ldots\ldots\ldots (2)$$

Where, Dd = Drainage Density Index (km/km^2), ΣL= Total River Length (km), A = Catchment Area (Km^2).

According to Sukiyah et al. (2009), drainage density (Dd) values are categorized into five distinct levels that reflect the geomorphological and geological characteristics of a landscape. Values classified as very coarse (less than 1.24) and coarse (1.24 to 2.49) typically indicate regions characterized by coarse rock textures, with relatively low erosion rates and minimal tectonic influence. As the density increases to the medium category between 2.49 and 3.73, it represents a medium rock texture where the topography begins to be significantly shaped by tectonic activities. Furthermore, higher values representing fine textures from 3.73 to 4.97 and very fine textures exceeding 4.97 describe terrains that are heavily influenced by the complex interplay of intensive erosion and active tectonics. Consequently, this parameter serves as a vital analytical tool for evaluating the surface texture, drainage system efficiency, and overall environmental conditions within the study area.

3.1.4 Form Factor (Rf), Ratio of Circularity (Rc), and Ratio of Elongation (Re)

In watershed morphometric analysis, there are three parameters used to understand the physical shape of watersheds that affect water flow response, especially during rainfall, namely the form factor (Rf), ratio of circularity (Rc), and ratio of elongation (Re). The form factor is the ratio of the catchment area to the square of the catchment area (Horton, 1945). A perfectly circular watershed will always have a value of 0.7854 (Javed et al., 2009). The smaller the value, the more elongated (oval) the shape of the watershed, and if the opposite is true, the shape of the watershed will approach a perfect circle. Circular watersheds generally have short river flows (Kuldeep and Upsana, 2012; Winarto et al., 2019). The Rf value is calculated using Equation (3):

$$Rf = \frac{A}{Lb^2} \quad \ldots\ldots\ldots (3)$$

Where, Rf = Form Factor, A = catchment area (km^2), L_b^2 = catchment length / Length of main parent river (km).

The circularity ratio (Rc) is obtained from the ratio between the area of a watershed and the area of a circle with the same circumference as the watershed (Miller, 1953; Strahler, 1964). A low Rc value indicates an elongated watershed shape, while a high Rc value indicates a circular watershed shape (Kumar Rai et al., 2017). The lower the circularity ratio (Rc) value, the lower the risk of flash floods. Conversely, the higher the Rc value, the higher the risk of flash floods (Nasir et al., 2020). Several researchers classify Rc values < 0.5 as elongated or elongated watershed, and Rc values > 0.5 as rounded or circular watershed (Srinivasa Vittala et al., 2004; Vinutha and Janardhana, 2014; Kumar Rai et al., 2017). The Rc value is calculated using Equation (4):

$$Rc = \frac{4\pi A}{P^2} \quad \ldots\ldots\ldots (4)$$

Where, Rc = Circularity ratio, A = catchment area (km^2), p^2 = Catchment perimeter (km).

The elongation ratio (Re) is the ratio of the diameter of a circle in a watershed to the maximum length of the watershed (Schumm, 1956; Kumar Rai et al., 2017; Winarto et al., 2019). Schumm (1956) classifies the elongation ratio (Re) into 5 categories, namely Circular (0.9-1.0), oval (0.8-0.9), less elongated (0.7-0.8), elongated (0.5-0.7), and more elongated (< 0.5). A high Re value indicates a circular watershed shape, resulting in high infiltration rates and low run-off. Conversely, a low Re value indicates an elongated watershed shape, resulting in low infiltration rates and high run-off (Balasubramanian et al., 2017). The Re value is calculated using Equation (5):

$$Re = 2\sqrt{(A/\pi)} / Lb \quad \ldots\ldots\ldots (5)$$

Where, Re = Elongation ratio, A = Catchment area (km^2), Lb = Catchment length / Length of main parent river (km).

3.2 Hydrological Analysis

Hydrological analysis is a combination of descriptions of hydrological phenomena such as rainfall or precipitation, temperature, evaporation, duration of sunshine, wind speed, river discharge, and water level, which constantly change over time. For certain purposes, hydrological data can be collected, calculated, presented, and interpreted using specific procedures (Yuliana, 2008). The hydrological parameters or components analyzed are as follows:

3.2.1 Rainfall/ Precipitation

Precipitation is the fall of water from the atmosphere to the earth's surface in the form of rain, snow, fog, dew, and hail. Rain causes river discharge to increase rapidly and expands the catchment area, which leads to quick surface runoff. In this study, the algebraic arithmetic method was used for rainfall analysis. The stations involved in this method's calculations could be located within the watershed itself or outside but nearby. Algebraic arithmetic calculations were performed using Equation (6). Algebraic arithmetic calculations were performed using Equation (6):

$$P = (P1+P2+\cdots+Pn)/n \quad \ldots\ldots\ldots (6)$$

Where, P = Average rainfall in the area, P1, P2, ..., Pn = Rainfall at observation points, n = number of stations.

3.2.2 Rainfall Data Series Testing (RAPS)

Before rainfall data is used for further calculations, it must first undergo consistency testing. This consistency test is to verify the accuracy of field data that is not affected by errors during transmission or measurement; the data must describe hydrological phenomena as they actually occur in the field (I Made Kamiana, 2011). Rainfall data consistency testing is performed using the Rescaled Adjusted Partial Sums (RAPS) method. This method shows rainfall data consistency with cumulative deviation values from the average value based on Equations (7-10):

$$Sk^* = \sum_{i=1}^{k}(Yi - Y) \quad \ldots\ldots\ldots (7)$$

$$Y = \frac{\sum Yi}{N} \quad \ldots\ldots\ldots (8)$$

Where k = 1, 2,… N; when k = 0, then Sk*= 0

$$Dy^2 = \sum_{i=1}^{k}(\frac{(Yi-Y^2}{N}) \quad \ldots\ldots\ldots (9)$$

$$Sk^{**} = \frac{Sk^*}{Dy} \quad \ldots\ldots\ldots (10)$$

Where, Sk* = cumulative deviation value from the mean value, Yi = i-th Y data value, Y = mean Y value, N = number of Y data, Sk** = Rescaled Adjuster Partial Sums (RAPS), Dy = standard deviation of the Y data series.

After Sk** is obtained for each k, calculate the values of Q and R using Equation (11):

$$Q = |Sk^{**}|max \text{ or } R = Sk^{**} max - Sk^{**} min \quad \ldots\ldots\ldots (11)$$

Next, compare the amount of data (N) and a certain confidence level (a). If Calculated Q < Critical Q or Calculated R < Critical R, then the data series analyzed is consistent.

3.2.3 Evapotranspiration

Evapotranspiration is evaporation from land surfaces covered with soil and vegetation (Kyatengerwa et al., 2020). The evapotranspiration calculation method of Thornthwaite (1948) is commonly used in Indonesia (Baskoro et al., 2024). The Thorntwaite method of calculating evapotranspiration requires only air temperature (Azizah et al., 2023). Evapotranspiration calculations using the method of Thornthwaite (1948), in accordance with the literature from Triatmodjo (2008) and Gode et al. (2020) are performed using Equations (12-15):

$$I = \sum 12/(m=1)\ (Tm/5)1.514 \quad \ldots\ldots\ldots (12)$$

$$ET_{month} = 1.62\ ((10.Tm)/I)a \quad \ldots\ldots\ldots (13)$$

$$a = 675.10\text{-}09\ I3 - 771.\ 10\text{-}7\ I2 + 179.\ 10\text{-}4.\ I + 0.492 \quad \ldots\ldots\ldots (14)$$

$$ET_{correction} = ET_{monthly}.\ Correction\ Factor \quad \ldots\ldots\ldots (15)$$

Where, ET_{month} = Evapotranspiration monthly (cm), Tm = Average monthly temperature (°C), and I = Annual heat index.

3.2.4 Run-Off Coefficient (C)

The surface run-off coefficient is the ratio between surface run-off and rainfall in a watershed (Kartiwa and Irianto, 2012). The magnitude of the surface run-off coefficient can describe the criticality of a watershed, especially its hydrological conditions. The average run-off coefficient in this study was calculated based on land cover type, slope, and soil type according to Mahmoud and Alazba (2015), as shown in Table 1. To determine the Cro value for an area, use Equation (16):

Table 1: Run-Off coefficient values based on land cover, land type, and slope gradient (Mahmoud and Alazba, 2015).

Land Use	Slope (%)	Sand	Loamy Sand	Sandy Loam	Loam	Silt Loam	Silt	Sandy Clay Loam	Clay Loam	Silty Clay Loam	Sandy Clay	Salty Clay	Clay
Forest	< 0.5	0.03	0.07	0.10	0.13	0.17	0.20	0.23	0.27	0.30	0.33	0.37	0.40
	0.5 - 5	0.07	0.11	0.14	0.17	0.21	0.24	0.27	0.31	0.34	0.37	0.41	0.44
	5 - 10	0.13	0.17	0.20	0.23	0.27	0.30	0.33	0.37	0.40	0.43	0.47	0.50
	> 10	0.25	0.29	0.32	0.35	0.39	0.42	0.45	0.49	0.52	0.55	0.59	0.62
Grass	< 0.5	0.13	0.17	0.20	0.23	0.27	0.30	0.33	0.37	0.40	0.43	0.47	0.50
	0.5 - 5	0.17	0.21	0.24	0.27	0.39	0.34	0.37	0.41	0.44	0.47	0.51	0.54
	5 - 10	0.23	0.27	0.30	0.33	0.27	0.40	0.43	0.47	0.50	0.53	0.57	0.60
	> 10	0.35	0.39	0.42	0.45	0.31	0.52	0.55	0.59	0.62	0.65	0.69	0.72
Crop	< 0.5	0.23	0.27	0.30	0.33	0.37	0.40	0.43	0.47	0.50	0.53	0.57	0.60
	0.5 - 5	0.27	0.31	0.34	0.37	0.41	0.44	0.47	0.51	0.54	0.57	0.61	0.64
	5 - 10	0.33	0.37	0.40	0.43	0.47	0.50	0.53	0.57	0.60	0.63	0.67	0.70
	> 10	0.45	0.49	0.52	0.55	0.59	0.62	0.65	0.69	0.72	0.75	0.79	0.82
Bare Soil	< 0.5	0.33	0.37	0.40	0.43	0.47	0.50	0.53	0.57	0.60	0.63	0.67	0.70
	0.5 - 5	0.37	0.41	0.44	0.47	0.51	0.54	0.57	0.61	0.64	0.67	0.71	0.74
	5 - 10	0.43	0.47	0.50	0.53	0.57	0.60	0.63	0.67	0.70	0.73	0.77	0.80
	> 10	0.55	0.59	0.62	0.65	0.69	0.72	0.75	0.79	0.82	0.85	0.89	0.92
IMP	-	1.00	1.00	1.00	1.00	1.00	1.00	1.00	1.00	1.00	1.00	1.00	1.00

$$Cro| = (A1.C1+A2.C2+\cdots+An.Cn)/(A1+A2+\cdots+An) \quad \ldots\ldots\ldots (16)$$

Where, Cro = Surface run-off coefficient of the watershed, Ci = Surface run-off coefficient of land cover type I, Ai = Area of land cover with land cover type I.

3.2.5 Watershed Water Balance Calculation

The water balance calculation is performed by combining all hydrological components that have been calculated in the previous stage, namely rainfall (precipitation), evapotranspiration, infiltration, and run-off. All calculations use consistent units in mm/year and are converted to discharge in m^3/year based on the area of each watershed.

Annual precipitation is calculated as the total amount of monthly rainfall in a year, calculated using Equation (17):

$$P_{year} = \sum_{i=1}^{12} Pi \text{ (mm/year)} \quad \ldots\ldots\ldots (17)$$

After that, the P_{year} value will be converted into precipitation discharge, calculated using the following Equation (18):

$$P_{discharge} = P_{year} \text{ (m/year) x A} \quad \ldots\ldots\ldots (18)$$

Where, $P_{discharge}$ = Discharge Precipitation (m^3/year), P_{year} = Total annual Precipitation (mm/year or m/year), Pi = Precipitation in i-month, A = Watershed area (m^2).

Next, evapotranspiration is calculated using the method of Thornthwaite (1948) based on monthly temperatures (Equation 13). The annual evapotranspiration value is expressed in mm per year and then converted into discharge, which is calculated using Equation (19):

$$ET_{discharge} = ET_{year} \text{ (m/year) x A} \quad \ldots\ldots\ldots (19)$$

Next, calculate the effective precipitation, which is the rainfall that has the potential to become surface run-off and infiltration. Effective precipitation is calculated using Equation (20):

$$P_{effective} = P_{year} - E_{year} \quad \ldots\ldots\ldots (20)$$

Where, $P_{effective}$ = Effective precipitation (mm/year or m/year), $P_{effective}$ discharge = Effective precipitation discharge (m^3/year), A = Watershed area (m^2)

Next, the run-off value is calculated based on the value of C land cover in the watershed (Equation 14). The run-off value obtained is then converted into run-off discharge calculated using Equation (21):

$$Q_{run\text{-}off} = P_{effective} \text{ (m/year) x C x A} \quad \ldots\ldots\ldots (21)$$

Where, $Q_{run\text{-}off}$ = Run-Off discharge (m^3/tahun), C = Run-off coefficient, A = Watershed Area (m^2).

Next, the infiltration value is calculated from the difference between the effective precipitation discharge and the run-off discharge, which is calculated using Equation (22):

$$Q_{infiltration} = P_{effective} - Q_{run\text{-}off} \quad \ldots\ldots\ldots (22)$$

Where, $Q_{infiltration}$ = Infiltration discharge (m^3/year), $P_{efektif\ debit}$ = Effective precipitation discharge (m^3/year), $Q_{run\text{-}off}$ = Run-off discharge (m^3/ year).

Next, the water balance value is calculated by combining the components of precipitation discharge, evapotranspiration discharge, infiltration discharge, and run-off discharge. The total water balance is written based on the relationship in Equation (23):

$$P_{discharge} = ET_{discharge} + Q_{Run\text{-}off} + Q_{Infiltration} \quad \ldots\ldots\ldots (23)$$

Where, $P_{discharge}$ = Precipitation discharge, $ET_{discharge}$ = Evapotranspiration discharge, $Q_{Run\text{-}off}$ = Run-off discharge, $Q_{Infiltration}$ = Infiltration discharge.

These results are presented in tabular form and as percentage graphs for the Wai Ruhu watershed.

4. Results

4.1 Watershed Morphometric Analysis

4.1.1 Stream Order

The river branching level is an index that indicates the number of tributaries flowing into the main river (Maimunah et al., 2020). Based on the results of GIS analysis, the Wai Ruhu watershed has stream orders ranging from order 1 to order 4. Details of the length of each order can be seen in Table 2,

while the spatial distribution of river orders can be seen in Fig. 4.

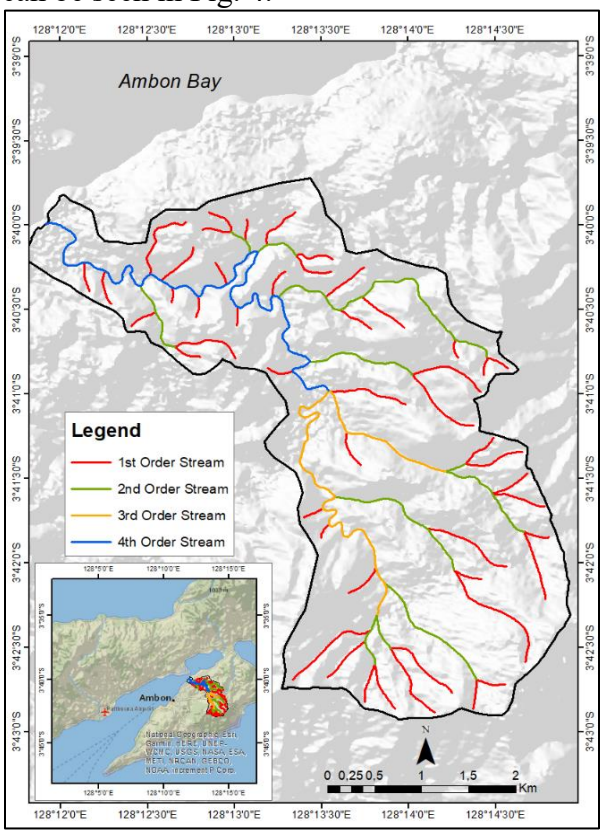

Fig. 4. Stream Order Map of the Wai Ruhu Watershed.

The total length of the rivers in the Wai Ruhu watershed is 47.9 km, with a tendency for the length to increase in higher-order rivers. Although order 1 has the most segments, its total length is relatively smaller than the other orders. Order 4 rivers, as the main river channels, have the longest individual lengths and therefore play an important role in channeling the accumulated flow from the entire watershed to the downstream area. The conditions indicate that the river network structure of the Wai Ruhu watershed has the potential to accelerate the flow concentration time in the main river, which has implications for increased peak discharge and flood risk in the downstream area. To test the statistical significance of the differences in river length between orders, a Kruskal-Wallis test was performed, as shown in Fig. 5.

This non-parametric approach was selected because the stream morphometric data in the Wai Ruhu watershed do not follow a normal distribution, characterized by significant outliers and a sharp asymmetrical distribution across different orders. From a hydrological perspective, this reflects extreme spatial variability. The headwater regions are dominated by numerous but short 1st and 2nd-order segments, while the downstream area is characterized by fewer but significantly elongated higher-order channels.

The variation in segment length is strongly dictated by the lithological control along the flow path. In the upstream reaches, the presence of resistant ultramafic and volcanic rocks limits lateral erosion, resulting in a fragmented and short river network. Conversely, as the river enters the downstream zone, which serves as a sediment sink consisting of alluvium and loose coral limestone, the resistance to fluvial scouring decreases significantly. These unconsolidated geological conditions allow the high-order river (4th order) to develop more freely and extend its length through meandering processes across the alluvial plains.

The Kruskal-Wallis test results show a p-value < 0.05 ($p = 0.0029$) with $X^2 = 13.95$ ($df = 3$), statistically confirming that the differences in segment length between orders are not coincidental but are a result of the complex interaction between stream hierarchy and geological formations. This finding aligns with Horton's Law of Stream Lengths, where an increase in stream order is geometrically proportional to an increase in segment length. Practically, the accumulation of flow in the long 4th-order segments over the downstream sediment layers increases the time of concentration (Tc) while simultaneously raising the risk of river overflow in these low-lying areas.

4.1.2 Results of Ratio of Bifurcation (Rb)

Based on the calculations in Table 4, the Rb value varies between 0.56 and 2.56. Referring to the classification (Verstappen, 1983), this value indicates that the Wai Ruhu watershed has undergone deformation due to tectonic movements and volcanic activity in the past. This is reinforced by the geological conditions in Fig. 3, where the study area is

dominated by deformed volcanic rocks. Physical evidence presented through the Rose Diagram (Figs. 7a, b) shows the existence of clear structural control through the dominance of the orientation of ridges (NE-SW) and valleys (NW-SE), as can be seen in Fig. 6.

Table 2: Stream Order in the Wai Ruhu Watershed.

Order – n	Number	Length (km)
1	49	23.996
2	11	11.430
3	2	5.618
4	1	6.832
Total	63	47.877

Table 3: Results of the Kruskal-Wallis test for river length between orders in the Wai Ruhu watershed.

Kruskal-Wallis chi-squared	13.951
df	3
p-value	0.002972

Table 4: Recapitulation of bifurcation ratio index in Wai Ruhu Area.

Rb 1_2	Rb 2_3	Rb 3_4	Classification
2.1	2.56	0.56	Deformed

This branching ratio is influenced by rock type and local geological structure. In line with research (Usman and Hamim, 2018), the use of geospatial analysis is very important to understand how geological impacts affect river networks. In the Wai Ruhu watershed, the volcanic rock types of Ambon and coral limestone indicate that although these rocks are easily eroded and form many tributaries, their flow direction remains locked in weak zones (faults). This explanation is supported by the fact that this lithology has low permeability and limited water absorption in massive areas, thereby strengthening the potential for surface run-off (Howard, 1967; Langbein, 1964).

Hydrologically, an Rb value < 3 reflects the characteristic of a very rapid rise in flood water levels followed by a rapid decline (Soewarno, 1991). Thus, it can be concluded that the synchronicity between the low Rb value and the straightness pattern on the Rose Diagram proves that the tectonic structure of the Banda Inner Arc actively controls the architecture of the river network in the Wai Ruhu watershed. This condition increases the vulnerability of the watershed to flooding, given that water will concentrate more quickly towards the main channel that follows these fault lines.

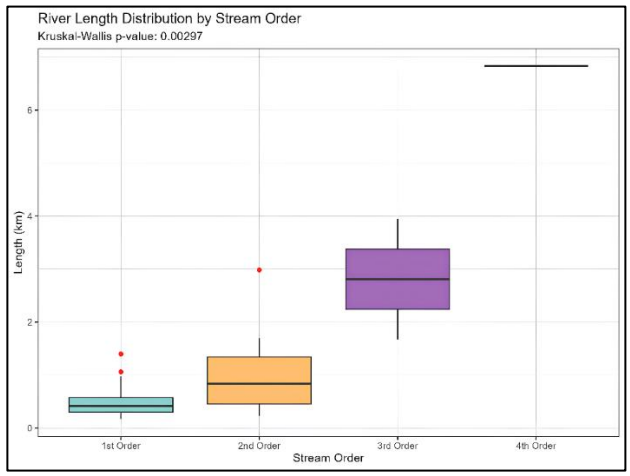

Fig. 5. Boxplot of River Length by Order in the Wai Ruhu Watershed.

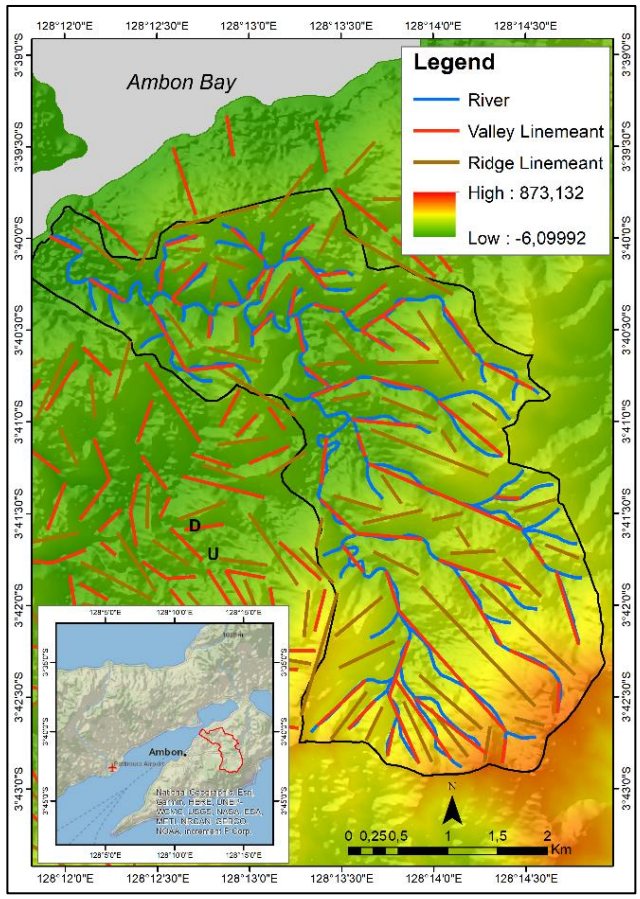

Fig. 6. Map of Ridge and Valley Alignment.

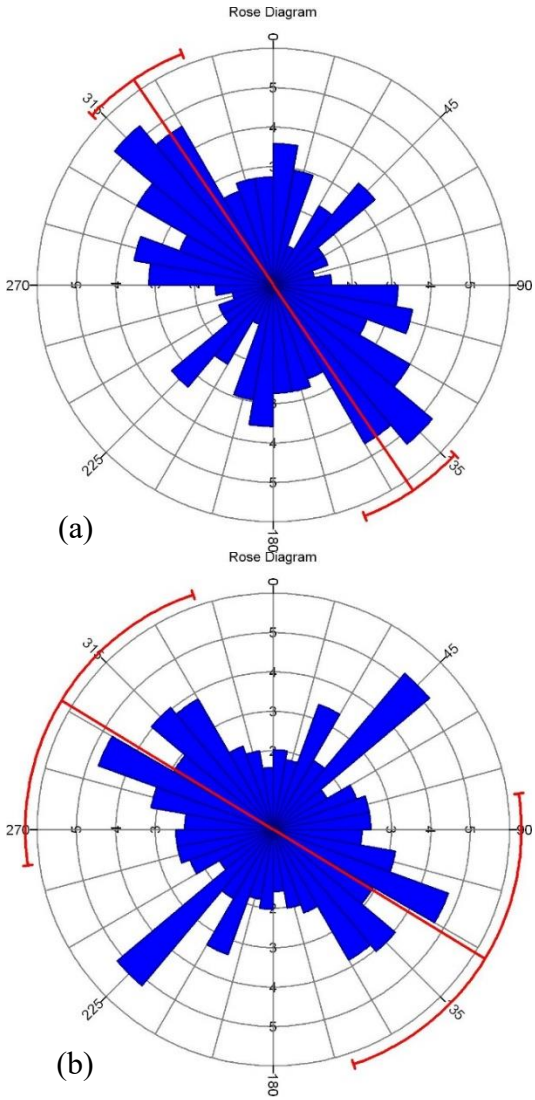

Fig. 7. Rose diagram showing the straightness of the valley (a) and the straightness of the ridge (b) in the Wai Ruhu watershed.

Table 5: Drainage density value in the Wai Ruhu watershed.

Dd	**According to** (Sukiyah et al., 2009)
3.0	Medium

4.1.3 Drainage density (Dd)

Drainage density (Dd) was first introduced by Horton (1945) and its use has been reinforced in hydrological disaster analysis (Rudraiah et al., 2008). The Dd value is greatly influenced by lithology, soil texture, slope, rainfall, and vegetation cover, and is closely related to the potential for run-off and flood risk in an area.

Drainage density (Dd) is the ratio between the total length of rivers and the area of the watershed (Horton, 1945). The drainage density value of a watershed is generally influenced by the resistance of bedrock to weathering, the permeability of the overlying rock, climate, and vegetation (Javed et al., 2009). A low drainage density value indicates that the area has rocks with high permeability and coarse drainage texture, while a high value indicates the opposite (Van Zuidam, 1985; Sukiyah, 2017). In addition, drainage density can also represent the hardness of rocks, where rocks with low Dd values tend to be harder and more resistant than rocks with high Dd values (Sukiyah, 2012).

Based on the data in Table 5, the Dd value of the Wai Ruhu watershed is classified as moderate according to Sukiyah et al. (2009). These figures illustrate the varying hydrological response in each lithological zone along the watershed. The upstream part of this area is dominated by massive ultramafic (JKu) rocks that are highly resistant to physical weathering. This factor, combined with the presence of primary and secondary dryland forest vegetation on crystalline rocks with steep slopes, limits the formation of river channels. The land cover and topography conditions in the upper reaches can be seen in Fig. 8. Although these rocks tend to be impermeable (low permeability), their extreme hardness means that the Dd value in the upper reaches does not develop densely due to the resistance of the rocks to erosion.

Fig. 8. Upper part of the WaiRuhu Watershed.

Fig. 9. Downstream Wai Ruhu Watershed.

In the middle part of the watershed, the lithology consists of Ammonite rock, which is more susceptible to weathering than the ultramafic rock upstream. This softer lithology, combined with land cover consisting of scrub and mixed dryland agriculture, triggers the formation of denser river channels (medium texture). This middle region is the main contributor to the watershed's flow density, where the flow more easily erodes weathered volcanic material.

Finally, the downstream section, which is dominated by alluvial lithology, should theoretically provide good infiltration space. However, its geographical position, directly adjacent to the sea, as shown in Fig. 9, has a very flat slope (0%), causing rapid groundwater saturation. Although a Dd value of 3.0 indicates a well-established drainage system, the presence of backwater (the effect of tidal fluctuations that impede river flow) and fine sand deposits causes a sharp decline in drainage efficiency, which ultimately triggers overflow and flooding.

4.1.4 Form Factor (Rf), Ratio of Circularity (Rc), and Ratio of Elongation (Re)

The parameter calculation results in Table 6 show a form factor (Rf) value of 0.3511, a circularity ratio (Rc) of 0.4, and an elongation ratio (Re) of 0.1. The Re value falls into the more elongated category. This condition is supported by the Rf value, which is well below 0.7854. According to Javed et al. (2009), this confirms that a highly elongated DAS shape will cause water flow to reach its peak more slowly but have a longer flow duration.

Table 6: Form Factor (Rf), Ratio of Circularity (Rc), and Ratio of Elongation (Re) Values in the Wai Ruhu Watershed.

Rf	Rc	Re
0.3511	0.4	0.1

This elongated watershed has a direct impact on hydrological conditions, especially in the downstream area. According to Balasubramanian et al. (2017), a low Re value indicates low infiltration rates and high surface run-off. In downstream areas, the elongated shape causes water from the entire watershed area to collect and flow through the same main channel for a long period of time. As a result, the downstream area receives a large accumulation of water continuously.

Although an Rc value of 0.4 indicates a lower risk of flash flooding compared to rounded watersheds, the elongated characteristics of this watershed actually trigger flooding downstream. This is exacerbated by the very flat topography downstream with a slope of 0%, as can be seen in Fig. 9. Water accumulation from this elongated watershed cannot be directly drained into the sea, especially when the soil is already saturated with water. This phenomenon causes the downstream drainage system to exceed its capacity, making flooding an inevitable phenomenon in the area.

4.2 Hydrological Analysis

4.2.1 Rainfall/ Precipitation

Based on Table 7, monthly rainfall statistics for the period 2014-2024 were obtained from the Pattimura Meteorological Station through the database portal database of Badan Meteorologi, Klimatologi, dan Geofisika (2024) shows that the study area has high rainfall intensity but with inconsistent seasonal patterns.

These hydrometeorological characteristics are in line with the geographical conditions of Ambon City, a small volcanic island in the Maluku Islands. This phenomenon is significantly influenced by the mountainous topography of the region and its geographical location, which borders directly on the sea, triggering local climate variability (Sinay et al., 2020).

Based on the results of rainfall data processing for the 2014–2024 period, the average annual rainfall value presented in Fig. 10 is 3,607.5 mm/year. This value falls into the very high category, indicating that the study area has abundant rainfall potential throughout the year. This is consistent with the visualization of total annual rainfall in Fig. 11.

A more in-depth analysis of monthly fluctuations shows that the highest average rainfall occurs in July, with an accumulation over 11 years of 7,524.9 mm (average of 684.1 mm/month). Conversely, the lowest rainfall was recorded in November with a total accumulation of 845.4 mm and a monthly average of 76.9 mm.

4.2.2 Rainfall Data Series Testing (RAPS)

The results of the rainfall data consistency test at Pattimura Station using the RAPS (Rescaled Adjusted Partial Sums) method are presented in Table 8. Based on the calculation results, a Qmax value of 0.77072 with $Q/\sqrt{N} = 0.23$ was obtained.

Referring to the RAPS table, according to Sri Harto Br (1993), for a data count of n = 1 and a confidence level of 95%, a critical Q value of 1.14 is obtained. Since the $Q/\sqrt{N}$ value is smaller than the critical Q ($0.23 < 1.14$), the rainfall data for the 2014–2024 period is declared consistent. These results indicate that there are no significant changes in the data recording pattern, so the data is valid and suitable for further analysis.

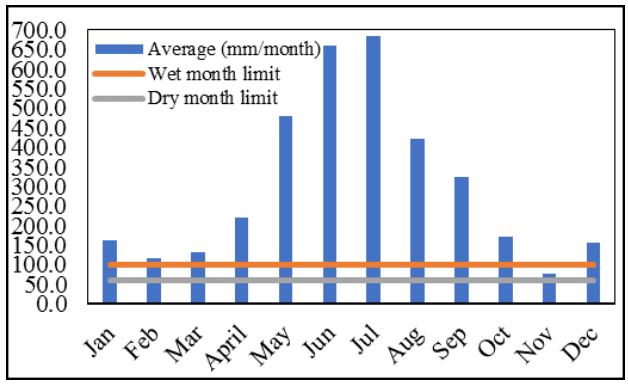

Fig. 10. Average Rainfall 2014 - 2024 at the Meteorological Station.

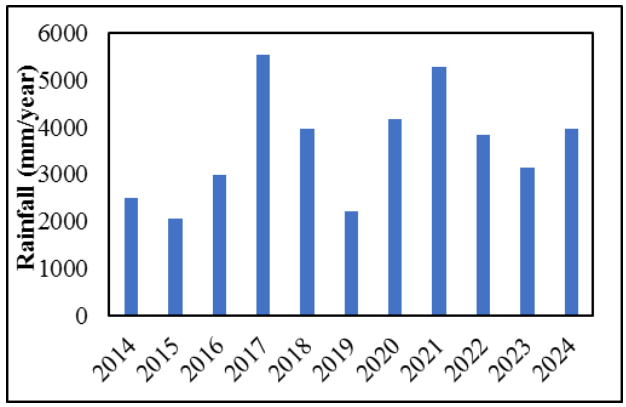

Fig. 11. Annual total rainfall 2014-2024 at the Meteorological Station.

Table 7: Monthly Rainfall Statistics at Pattimura Meteorological Station 2014 - 2024.

Rainfall 2014–2024													
Description	**Jan**	**Feb**	**Mar**	**Apr**	**May**	**Jun**	**Jul**	**Aug**	**Sep**	**Oct**	**Nov**	**Dec**	**Total (mm/year)**
Total/Sum	1799.2	1275.2	1438.8	2428.3	5292.9	7266.4	7524.9	4640.4	3571.6	1874.8	845.4	1724.2	39682.1
Average (mm/month)	163.6	115.9	130.8	220.8	481.2	660.6	684.1	421.9	324.7	170.4	76.9	156.7	3607.5
Max (mm/month)	302.3	195.6	209.2	354.8	827.9	1429.3	1336.7	924.4	653.7	442.9	181.6	266.4	7124.8
Min (mm/ month)	32.3	33.5	0	104.6	145.7	198.6	167.6	70.3	2.8	29.7	13.6	14.2	812.9

Table 8: RAPS Consistency Test Results for Annual Rainfall Data (2014 – 2024).

No	**y**	**$y - \bar{y}$**	**$(y - \bar{y})^2$**	**Sk***	**Dy^2**	**Sk****
1	482.9	-401.75	161399.41	-401.75	87046.422	-1.36168
2	659.2	-225.45	50825.65	-627.19	87046.422	-2.12581
3	925.5	40.85	1669.09	-586.34	87046.422	-1.98734
4	1429.3	544.65	296648.57	-41.68	87046.422	-0.14128
5	789.1	-95.55	9128.93	-137.23	87046.422	-0.46512
6	578.5	-306.15	93725.04	-443.37	87046.422	-1.50277
7	838.2	-46.45	2157.18	-489.82	87046.422	-1.66020
8	1336.7	452.05	204353.31	-37.76	87046.422	-0.12800
9	1149.8	265.15	70306.93	227.39	87046.422	0.77072
10	627.0	-257.65	66381.18	-30,25	87046.422	-0.10255
11	914.9	30.25	915.34	0.00	87046.422	0.00000
$\bar{y}$	884.6454545	$\sum(y - \bar{y})^2$	957510.65		Qmax	0.77072
$Q/\sqrt{n}$ =	0.23	<	$Q_{critical}$ =	1,14		Consistent

4.2.3 Evapotranspiration calculation

Based on the calculations in Table 9, the annual evapotranspiration value in the Ambon Island region is 1,673.48 mm/year. This value is used to calculate effective precipitation, which is obtained from the difference between annual rainfall and the evapotranspiration value. Next, this effective precipitation value is multiplied by the watershed area to determine the effective precipitation discharge.

4.2.4 Run-Off Calculation (C)

The determination of the average run-off coefficient value is based on two main parameters, namely slope gradient and land cover type. In the Wai Ruhu watershed, slope gradient is classified into five classes to provide a detailed topographical description, namely: Flat (0-8%), Gentle (8-15%), Moderately Steep (15-25%), Steep (25-45%), and Very Steep (>45%). This classification aims to map the topographical characteristics of the area that will affect the surface flow rate or run-off along the watershed area.

Based on the overlay results between the slope map (Fig. 12) and the land cover map (Fig. 13), each land unit was given a run-off coefficient (C) value referring to the standard (Mahmoud and Alazba, 2015). Due to differences in slope categories between the visual map and the reference table, data alignment was performed. Slope classes on the map with values above 10% (moderately steep to very steep) were adjusted to the >10% category in Table 2 to determine their coefficient values. The area of each land unit was calculated in square kilometers (km^2), which was then multiplied by the respective run-off coefficient value to obtain the total surface run-off contribution (C x Area). A recapitulation of the results of the calculation of land area and run-off coefficient values in the Wai Ruhu watershed is presented in detail in Table 9.

Based on the land cover map (Fig. 13), the upper to middle reaches of the Wai Ruhu watershed are dominated by dryland forests. This area is located on steep slopes, where Table 10 shows that primary and secondary dryland forests on slopes >10% contribute C x Area values of 0.68 and 0.55, respectively. In addition, scrub vegetation on steep slopes also contributes a high run-off value of 1.35. In the downstream part of the watershed, the map shows a concentration of dense settlements around the main river. In line with this data, the settlement class recorded the highest C x Area value of 3.46. This indicates that residential areas have a very significant influence on the volume of residential run-off in this watershed. Overall, the combination of steep slopes and land cover characteristics causes the Wai Ruhu watershed to have an average run-off coefficient value of 0.54.

Table 9: Evapotranspiration calculation results.

Temperatur St. Meteorologi Pattimura 2014 - 2024												
Description	**Jan**	**Feb**	**Mar**	**Apr**	**May**	**Jun**	**Jul**	**Aug**	**Sep**	**Oct**	**Nov**	**Dec**
Total/Sum	1799.2	1275.2	1438.8	2428.3	5292.9	7266.4	7524.9	4640.4	3571.6	1874.8	845.4	1724.2
I	13.4	13.4	13.2	12.9	12.7	12.0	11.7	11.7	12.3	12.8	13.5	13.5
	152.96											
a	**3.842**											
ETo month (cm)	15.1	15.1	14.9	14.5	14.2	12.1	11.4	11.4	13.7	14.4	15.2	15.2
cm/m -> mm/m	151.10	151.05	149.28	145.48	142.37	121.46	113.53	113.61	136.98	144.24	152.11	152.27
Evapotranspiration (mm/year)	1,673.48											

Table 10: Land cover data for the Wai Ruhu watershed.

Land Cover of the Wai Ruhu Watershed (2019)			
Legend	**(C) Value**	**Area (km^2)**	**C*Area**
Primary Dryland Forest (<0,5 - 5%)	0.13	0.05	0.01
Primary Dryland Forest (5 - 10%)	0.23	0.52	0.12
Primary Dryland Forest (> 10%)	0.35	1.95	0.68
Secondary Dryland Forest (<0,5 - 5%)	0.13	0.02	0.00
Secondary Dryland Forest (5 - 10%)	0.23	0.29	0.07
Secondary Dryland Forest (> 10%)	0.35	1.56	0.55
Shrubland (<0,5 - 5%)	0.23	0.06	0.01
Shrubland (5 - 10%)	0.33	0.65	0.21
Shrubland (> 10%)	0.45	3.00	1.35
Settlement/Built-up Area	1	3.46	3.46
Savanna/Grassland (<0,5 - 5%)	0.23	0.00	0.00
Savanna/Grassland (5 - 10%)	0.33	0.04	0.01
Savanna/Grassland (> 10%)	0.45	0.28	0.12
Mixed Dryland Agriculture (<0,5 - 5%)	0.33	0.08	0.03
Mixed Dryland Agriculture (5 - 10%)	0.43	0.59	0.25
Total			8.72
Average			0.54

4.2.5 Water Balance Calculations

Quantitative analysis of the main components of the water balance in the Wai Ruhu watershed includes parameters such as precipitation, evapotranspiration, effective precipitation, run-off, and infiltration. These data provide an overview of the watershed's capacity to collect, absorb, and drain rainwater. The results of this analysis also show differences in hydrological characteristics that are significantly influenced by land cover and slope factors in the area.

The evapotranspiration process in the Wai Ruhu watershed causes water loss to the atmosphere of 1.67347904 m/year, which is equivalent to 265,914,162.8 m^3/year in volume. This value indicates that a significant portion of rainfall is lost due to evaporation and vegetation transpiration, thereby reducing the amount of water available for surface run-off and infiltration.

Effective precipitation reflects the actual amount of water that contributes directly to the hydrological process after evaporation is subtracted. In this case, the Wai Ruhu watershed produces an effective precipitation discharge of 364,630,477.7 m^3/year. This value represents the net water potential available in the watershed for both replenishing groundwater reserves and feeding rivers.

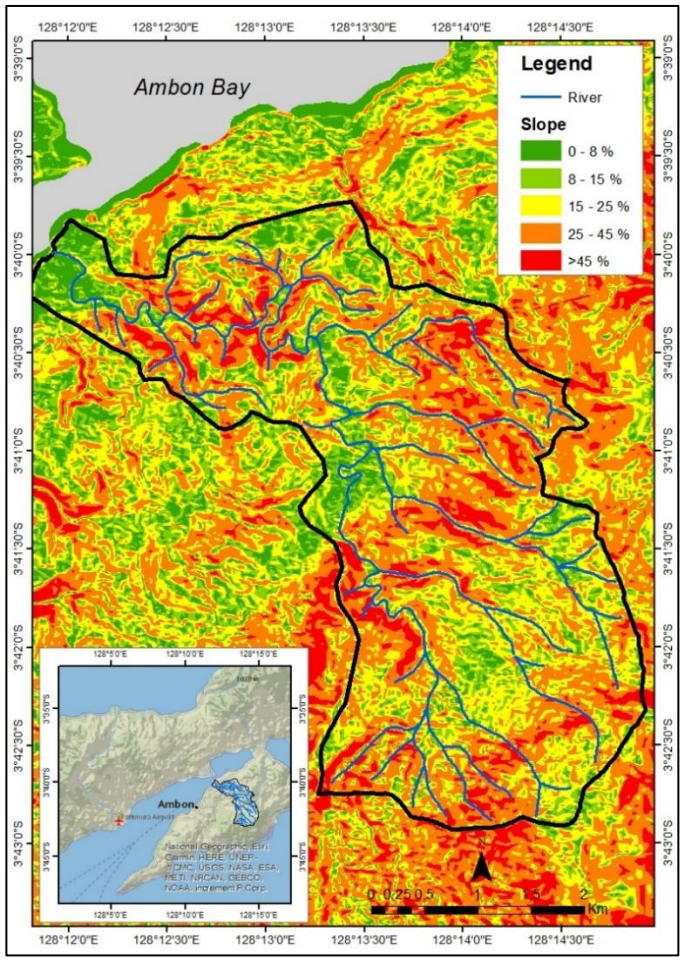

Fig. 12. Map of slope steepness in the Wai Ruhu Watershed.

Table 11: Results of water balance in Wai Ruhu Watershed.

Wai Ruhu Watershed	Watershed Area (m^2)	
	158,899,010	
	Precipitation (m/year)	Precipitation Discharge (m^3/year)
	3.96821	630,544,640.5
	Evapotranspiration (m/year)	Evapotranspiration Discharge (m^3/year)
	1.67347904	265,914,162.8
	Effective Precipitation (m/year)	Effective Precipitation Discharge (m^3/year)
	2.9473096	364,630,477.7
	Average Run-Off Coefficient (C)	Run- Off Discharge (m^3/year)
	0.54	198,704,594.2
	Infiltration Discharge (m^3/year)	
	165,925,883.5	

The physical characteristics of the Wai Ruhu watershed are reflected in the average run-off coefficient (C) value of 0.54. With this value, the volume of water flowing directly on the surface (run-off discharge) reaches 198,704,594.2 m^3/year. This C value indicates that more than half of the effective precipitation (54%) turns into surface run-off. This condition indicates that the dominance of high surface run-off in the Wai Ruhu watershed contributes to an increased risk of flooding.

Meanwhile, the volume of water that infiltrates into the ground (infiltration rate) is 165,925,883.5 m^3/year. Because the run-off rate is greater than the infiltration rate, the Wai Ruhu watershed has a more significant level of flood vulnerability. This indicates low land absorption capacity, so conservation efforts are needed to increase infiltration capacity and reduce surface run-off volume.

Based on the water balance analysis presented in Fig. 14, the total volume of water entering the Wai Ruhu watershed system comes entirely from annual precipitation of 630,544,640.5 m^3/year. The distribution of hydrological components of the total input shows that evapotranspiration is the largest portion, with a percentage of 42.17%. This high evapotranspiration rate is greatly influenced by the geographical conditions of Ambon as a small island and the relatively high average air temperature of 27.7°C (Table 9). This high and stable temperature triggers intensive evaporation on land before the water has time to be distributed further into the subsurface hydrological system or become subsurface run-off.

Furthermore, the surface run-off component accounts for 31.51%. This high value is a key indicator of the dominance of surface run-off, which contributes directly to an increased risk of flooding in the Wai Ruhu watershed.

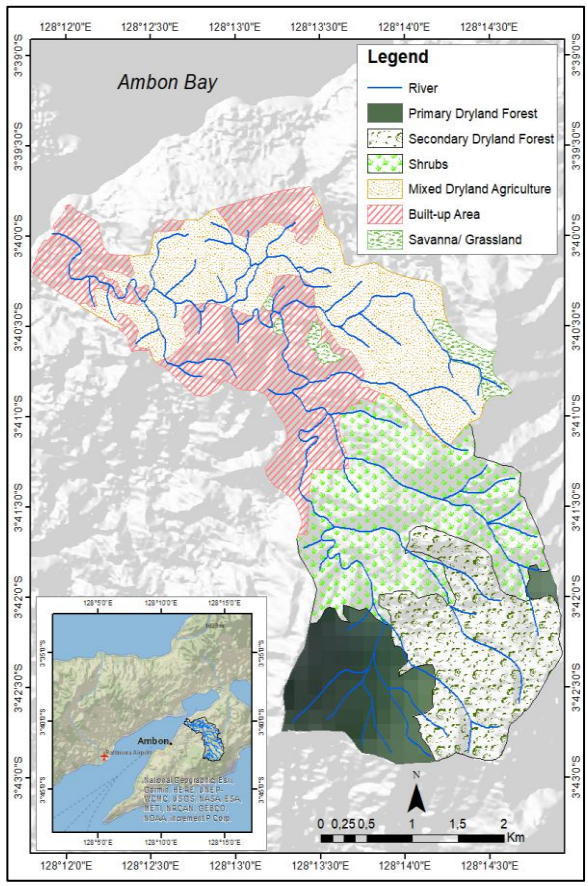

Fig. 13. 2019 land cover map of the Wai Ruhu watershed.

On the other hand, the infiltration component only accounts for 26.31%, which is the smallest portion of the entire water distribution system. Overall, the condition where run-off discharge is much greater than infiltration discharge confirms that the Wai Ruhu watershed has a significant level of flood vulnerability. This indicates low land absorption capacity, so appropriate conservation efforts are needed to increase infiltration capacity to reduce high surface run-off volume.

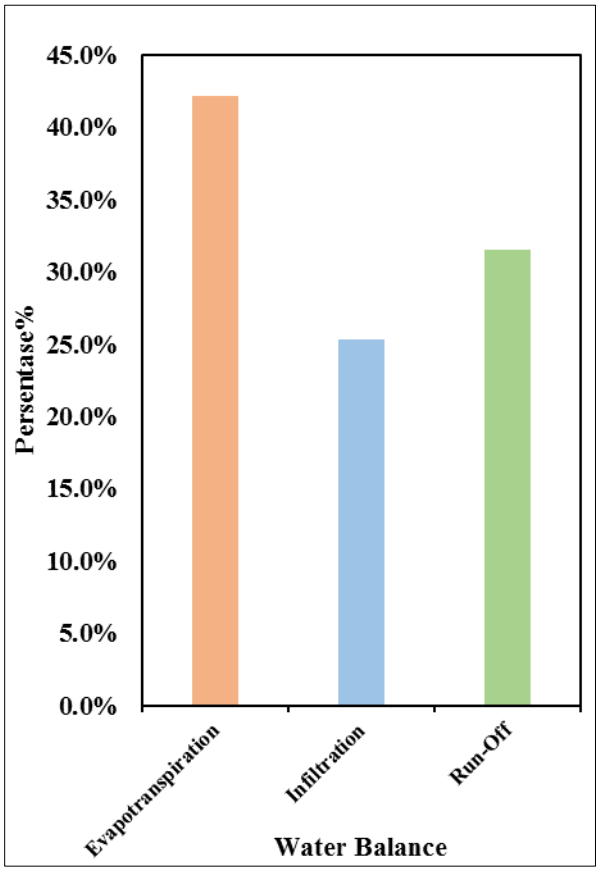

Fig. 14. Percentage of Water Balance Components to Precipitation Flow in the Wairuhu Watershed.

5. Discussion

The critical hydrological conditions in the Wai Ruhu watershed are a manifestation of the destructive interaction between extreme climatological loads and biophysical land characteristics. The exceptionally high annual rainfall (3,607.5 mm/year), with massive peak intensities, is not merely a statistical value but a hydrological load that exceeds the natural thresholds of small tropical islands (Sri Harto Br, 1993; Nunn, 2009; Sinay et al., 2020). Critical analysis reveals that the rapid flood response is triggered by the synergy between rainfall intensity (Terry and Kostaschuk, 2007) and an elongated watershed geometry (Re = 0.1, Rc = 0.4, Rf = 0.3511). Unlike circular watersheds, this elongated shape causes flows from the headwaters to the lowlands to reach the outlet simultaneously, creating a cumulative flooding phenomenon (Schumm, 1956; Gupta, 2017) that drastically shortens the time of concentration in urban areas.

The effectiveness of natural processes in reducing floods has proven to be minimal in this region. Although annual evapotranspiration reaches 1,673.48 mm/year, its role in reducing peak discharge is insignificant because, in humid tropical regions, rainfall variability is a far more dominant driver of surface water availability than evaporation (Padrón et al., 2020). This condition is exacerbated by the loss of infiltration capacity due to uncontrolled urban expansion downstream (C = 0.54), where land degradation and steep topography force effective precipitation to convert immediately into surface run-off (Horton, 1945; Strahler, 1957). This phenomenon underscores that conventional structural drainage solutions in Ambon City will inevitably reach a saturation point, as downstream drainage capacity is continuously overwhelmed by water volumes that the soil can no longer absorb (Wohl, 2010).

From a geological perspective, this accelerated flow is also strongly governed by structural factors. The low bifurcation ratio (Rb: 0.56–2.56) evidences a dominant tectonic control from the Banda Inner Arc, which efficiently directs the drainage network downstream (Howard, 1967; Verstappen, 1983). Variations in drainage density (Dd) due to lithological heterogeneity, where resistant rocks upstream limit channels while soft rocks in the middle trigger a dense network, create an accumulation of risk in coastal areas (Javed et al., 2009; Sukiyah, 2012). This risk peaks when massive river discharge is obstructed by the backwater phenomenon caused by

tidal fluctuations (Rudraiah et al., 2008; Ogden et al., 2011).

In conclusion, flood mitigation in the Wai Ruhu watershed can no longer rely solely on downstream civil engineering approaches. A paradigm shift toward strict upstream conservation zone management is required to compensate for the elongated watershed shape and to restore lost infiltration capacity. Integrating morphometric analysis with synthetic unit hydrograph modeling and the implementation of green infrastructure adaptive to fluvial marine dynamics is essential to ensure the sustainability of water resources and the safety of Ambon City from future flash flood threats.

6. Conclusions

This study confirms that the Wai Ruhu watershed is structurally predisposed to rapid hydraulic discharge. The dominance of tectonic control and straight river patterns significantly shortens the flow concentration time, causing extreme rainfall to convert almost instantaneously into peak discharge downstream. The core issue is not merely rainfall volume, but the inability of the lithology and land cover to facilitate infiltration, forcing the vast majority of precipitation into destructive surface run-off. The integration of morphometric and water balance data proves that flood vulnerability in Ambon City's densely populated areas is the result of a synergy between natural drainage efficiency (geological factors) and artificial infiltration barriers (urbanization). Based on these findings, watershed management strategies must shift from reactive impact handling to the following structural and regulatory interventions:

1. Morphometry-Based Land Use Regulation: Authorities must designate "Critical Morphological Zones" in areas with high drainage density (Dd). In these zones, land conversion should be strictly prohibited and transitioned into protected areas. Building Coverage Ratios (BCR) in the middle to downstream sectors must be tightened to ensure that green open spaces are not further eroded by residential expansion.
2. Infiltration Enhancement via Non-Structural Interventions: Given the limited natural infiltration due to lithological constraints, a "Zero Delta Q Policy" is mandatory. Every new development should require the installation of recharge wells, biopore holes, or retention tanks capable of absorbing rainfall volume proportional to the building's roof area. In downstream areas, conventional paving should be replaced with porous pavements to force water back into the ground.
3. Relevance and Optimization of Flood Early Warning Systems (EWS): Because the low bifurcation ratio (Rb) results in an extremely short flood response time, conventional warning systems are no longer sufficient. It is essential to install Automatic Weather Stations (AWS) and Automatic Water Level Recorders (AWLR) in the upstream areas, integrated in real-time with mobile alerts for residents. The narrow lag time demands evacuation protocols based on rainfall thresholds rather than waiting for riverbanks to overflow.

Acknowledgments

The authors would like to express their sincere gratitude to the Indonesia Endowment Fund for Education (LPDP), Ministry of Finance, Republic of Indonesia, for providing financial support through a scholarship program. We also acknowledge the Indonesian Agency for Meteorology, Climatology, and Geophysics (BMKG) for providing rainfall data used in this study. Special thanks are extended to the Laboratory of Geomorphology and Remote Sensing, Faculty of Geological Engineering, Universitas Padjadjaran, for their academic and technical support during the research process.

Authors' Contribution

Nabila K. Tuanany proposed the main concept, involved in data curation, formal analysis, investigation, methodology, resources, handled software, and

visualization, and prepared the original draft. Emi Sukiyah, involved in formal analysis, methodology, and resources, provided supervision, performed validation, review, and edited the manuscript. Boy Yoseph CSSSA, involved in formal analysis, methodology, resources, provided supervision, performed validation, review, and editing of the manuscript. Axl Manuhutu, involved in investigation, resources, software, and visualization, performed review and editing of the manuscript.

Conflicts of Interest

The authors declare no conflicts of interest.

References

Abdalla, F., Shamy, I. E., Bamousa, A. O., Mansour, A., Mohamed, A., & Tahoon, M. (2014). Flash Floods and Groundwater Recharge Potentials in Arid Land Alluvial Basins, Southern Red Sea Coast, Egypt. *International Journal of Geosciences*, *05*(09), 971–982. https://doi.org/10.4236/ijg.2014.59083

Alarifi, S. S., Abdelkareem, M., Abdalla, F., & Alotaibi, M. (2022). Flash Flood Hazard Mapping Using Remote Sensing and GIS Techniques in Southwestern Saudi Arabia. *Sustainability*, *14*(21), 14145. https://doi.org/10.3390/su142114145

Ali, S. A., Parvin, F., Pham, Q. B., Vojtek, M., Vojteková, J., Costache, R., Linh, N. T. T., Nguyen, H. Q., Ahmad, A., & Ghorbani, M. A. (2020). GIS-based comparative assessment of flood susceptibility mapping using hybrid multi-criteria decision-making approach, naïve Bayes tree, bivariate statistics and logistic regression: A case of Topľa basin, Slovakia. *Ecological Indicators*, *117*, 106620. https://doi.org/10.1016/j.ecolind.2020.106620

Ariyani, D., Purwanto, Muh. Y. J., Sunarti, E., Perdinan, P., & Juniati, A. T. (2024). Integrated flood hazard assessment using multi-criteria analysis and geospatial modeling. *Journal of Degraded and Mining Lands Management*, *11*(4), 6121–6134. https://doi.org/10.15243/jdmlm.2024.114.6121

Azizah, V., Cholidah, N. N. Z., Sari, R. R. A., Religi, M. D., & Masitoh, F. (2023). Analisis Evapotranspirasi Pada Waduk Bening di SubDAS Brantas. *Geomedia Majalah Ilmiah Dan Informasi Kegeografian*, *21*(1), 10–19. https://doi.org/10.21831/gm.v21i1.46327

Badan Meteorologi, Klimatologi, dan Geofisika. (2024). *Data Parameter Meteorologi (Curah Hujan dan Suhu) Stasiun Meteorologi Pattimura Tahun 2024*. https://dataonline.bmkg.go.id/

Bakker, E., Pattilouw, S., Tanikwele, D., Tuhumury, D., Ayal, C., & Ulorlo, V. (2023). Korelasi Data Citra Satelit Radar dan Geologi Untuk Analisis Deformasi Permukaan, Studi Kasus Gempa Ambon September 2019. *Jurnal Geosains Dan Remote Sensing*, *4*(1), 11–18. https://doi.org/10.23960/jgrs.2023.v4i1.100

Balasubramanian, A., Duraisamy, K., Thirumalaisamy, S., Krishnaraj, S., & Yatheendradasan, R. K. (2017). Prioritization of subwatersheds based on quantitative morphometric analysis in lower Bhavani basin, Tamil Nadu, India using DEM and GIS techniques. *Arabian Journal of Geosciences*, *10*(24), 552. https://doi.org/10.1007/s12517-017-3312-6

Bashir, B., & Alsalman, A. (2024). Flooding Hazard Vulnerability Assessment Using Remote Sensing Data and Geospatial Techniques: A Case Study from Mekkah Province, Saudi Arabia. *Water*, *16*(19), 2714. https://doi.org/10.3390/w16192714

Baskoro, A. Y., Suripin, S., & Suprapto, S. (2024). Analisis Evapotranspirasi Metode Penman Modifikasi Dan Thornthwaite Terhadap Pemodelan Debit Fj. Mock: Analysis Of Evapotranspiration Using Modified Penman And Thornthwaite Methods On Fj. Mock's Run-Off Modelling. *Media Ilmiah Teknik Sipil*, *12*(1), 39–50. https://doi.org/10.33084/mits.v12i1.6134

Bemmelen, R. W. van. (1949). *The Geology of Indonesia, Vol. IA: General Geology of Indonesia and Adjacent Archipelagoes.*

U.S. Government Printing Office. https://www.scirp.org/reference/referencespapers?referenceid=3633886

Dimple, D., Rajput, J., Al-Ansari, N., Elbeltagi, A., Zerouali, B., & Santos, C. A. G. (2022). Determining the Hydrological Behaviour of Catchment Based on Quantitative Morphometric Analysis in the Hard Rock Area of Nand Samand Catchment, Rajasthan, India. *Hydrology*, *9*(2), 31. https://doi.org/10.3390/hydrology9020031

Duque, L.-F., O'Donnell, G., Cordero, J., Jaramillo, J., & O'Connell, E. (2025). Analysis of the Potential Impacts of Climate Change on the Mean Annual Water Balance and Precipitation Deficits for a Catchment in Southern Ecuador. *Hydrology*, *12*(7), 177. https://doi.org/10.3390/hydrology12070177

Elkhrachy, I. (2015). Flash Flood Hazard Mapping Using Satellite Images and GIS Tools: A case study of Najran City, Kingdom of Saudi Arabia (KSA). *The Egyptian Journal of Remote Sensing and Space Science*, *18*(2), 261–278. https://doi.org/10.1016/j.ejrs.2015.06.007

Folharini, S., Vieira, A., Bento-Gonçalves, A., Silva, S., Marques, T., & Novais, J. (2022). Soil Erosion Quantification using Machine Learning in Sub-Watersheds of Northern Portugal. *Hydrology*, *10*(1), 7. https://doi.org/10.3390/hydrology10010007

Gentana, D., Sulaksana, N., Sukiyah, E., & Yuningsih, E. T. (2018). Index of Active Tectonic Assessment: Quantitative-based Geomorphometric and Morphotectonic Analysis at Way Belu Drainage Basin, Lampung Province, Indonesia. *International Journal on Advanced Science, Engineering and Information Technology*, *8*(6), 2460–2471. https://doi.org/10.18517/ijaseit.8.6.6089

Gode, D., Kurnianto, Y. F., & Kusumastuti, C. (2020). Perbandingan Nilai Evapotranspirasi Menggunakan Metode Thornthwaite Dan Blaney-Cridle Di Kabupaten Manggarai Barat, Kabupaten Sikka, Dan Kabupaten Flores Timur. *Jurnal Dimensi Pratama Teknik Sipil*, *9*(1), 64–69.

Gupta, A. (2017). Tropical Geomorphology. In D. Richardson, N. Castree, M. F. Goodchild, A. Kobayashi, W. Liu, & R. A. Marston (Eds), *International Encyclopedia of Geography* (1st edn, pp. 1–10). Wiley. https://doi.org/10.1002/9781118786352.wbieg0546

Hall, R. (2012). Late Jurassic–Cenozoic reconstructions of the Indonesian region and the Indian Ocean. *Tectonophysics*, *570–571*, 1–41. https://doi.org/10.1016/j.tecto.2012.04.021

Haryanto, E. T., Sukiyah, E., & Rendra, P. P. R. (2019). Implication of catchment morphometric on small river discharge of upper Citarik river, West Java. *The Indonesian Journal of Geography*, *51*(2), 224–230.

Hermawan, D., & Yushantari, A. (2010). *Geologi dan Geokimia Panas Bumi Daerah Pohon Batu, Provinsi Maluku.* (p. 68). Pusat Sumber Daya Geologi, Kelompok Penyelidikan Panas Bumi. http://geologi.esdm.go.id/perpustakaan/?p=show_detail&id=580

Honthaas, C., Réhault, J.-P., Maury, R. C., Bellon, H., Hémond, C., Malod, J.-A., Cornée, J.-J., Villeneuve, M., Cotten, J., Burhanuddin, S., Guillou, H., & Arnaud, N. (1998). A Neogene back-arc origin for the Banda Sea basins: Geochemical and geochronological constraints from the Banda ridges (East Indonesia). *Tectonophysics*, *298*(4), 297–317. https://doi.org/10.1016/S0040-1951(98)00190-5

Horton, R. E. (1945). Erosional Development Of Streams And Their Drainage Basins; Hydrophysical Approach To Quantitative Morphology. *Geological Society of America Bulletin*, *56*(3), 275. https://doi.org/10.1130/0016-7606(1945)56%255B275:EDOSAT%255D2.0.CO;2

Howard, A. D. (1967). Drainage Analysis in Geologic Interpretation: A Summation. *AAPG Bulletin*, *51 (11), 2246–2259*. https://doi.org/10.1306/5D25C26D-16C1-11D7-8645000102C1865D

I Made Kamiana. (2011). *Teknik perhitungan debit rencana bangunan air*. Graha Ilmu.

Javed, A., Khanday, M. Y., & Ahmed, R. (2009). Prioritization of sub-watersheds based on morphometric and land use analysis using remote sensing and GIS techniques. *Journal of the Indian Society of Remote Sensing*, *37*(2), 261–274. https://doi.org/10.1007/s12524-009-0016-8

Jaya, R., Murti, S. H., Adji, T. N., & Sulaiman, M. (2024). Relation of morphometric characteristics to land degradation in the Biyonga sub-watershed, Gorontalo Regency, Indonesia. *Journal of Degraded and Mining Lands Management*, *11*(2), 5263–5277. https://doi.org/10.15243/jdmlm.2024.112.5263

Kartiwa, B., & Irianto, G. (2012). Alternative Method for Calculating Runoff Coefficient Based on Discharge Simulation Model by Applying Unit Hydrograph Concept (Kali Kripik Sub Watershed Case Study). *Indonesian Soil and Climate Journal (Atau Jurnal Tanah Dan Iklim)*, (10). https://repository.pertanian.go.id/handle/123456789/13637

Kuldeep, P., & Upsana, P. (2012). Quantitative geomorphological analysis of a watershed of Ravi River Basin, HP India. *International Journal of Remote Sensing and GIS.*, *1*(1), 41–56.

Kumar Rai, P., Narayan Mishra, V., & Mohan, K. (2017). A study of morphometric evaluation of the Son basin, India using geospatial approach. *Remote Sensing Applications: Society and Environment*, *7*, 9–20. https://doi.org/10.1016/j.rsase.2017.05.001

Kyatengerwa, C., Kim, D., & Choi, M. (2020). A national-scale drought assessment in Uganda based on evapotranspiration deficits from the Bouchet hypothesis. *Journal of Hydrology*, *580*, 124348. https://doi.org/10.1016/j.jhydrol.2019.124348

Lewerissa, R., Sismanto, S., Setiawan, A., & Pramumijoyo, S. (2017). The Study of Geological Structures in Suli and Tulehu Geothermal Regions (Ambon, Indonesia) Based on Gravity Gradient Tensor Data Simulation and Analytic Signal. *Geosciences*, *8*(1), 4. https://doi.org/10.3390/geosciences8010004

Mahmoud, S. H., & Alazba, A. A. (2015). Hydrological Response to Land Cover Changes and Human Activities in Arid Regions Using a Geographic Information System and Remote Sensing. *PLOS ONE*, *10*(4), e0125805. https://doi.org/10.1371/journal.pone.0125805

Maimunah, M., Nurlina, N., & Tsabita, G. F. I. (2020). Analisis Karakteristik Morfometri DAS Maluka Menggunakan Citra Satelit Shuttle Radar Topography Mission. *Jurnal Geografika (Geografi Lingkungan Lahan Basah)*, *1*(1), 12–19.

Miller, V. C. (1953). *A Quantitative Geomorphic Study of Drainage Basin Characteristics in the Clinch Mountain area, Virginia and Tennessee* (Proj. NR 389-402, Tech Rep 3). Columbia University, Department of Geology, ONR.

Mohammed, A., Adugna, T., & Takala, W. (2018). Morphometric analysis and prioritization of watersheds for soil erosion management in Upper Gibe catchment. *Journal of Degraded and Mining Lands Management*, *06*(01), 1419–1426. https://doi.org/10.15243/jdmlm.2018.061.1419

Muliati, Y. (2020). *Analisis Data Curah Hujan yang Hilang Dengan Menggunakan Metode Aljabar dan Resiprokal.* Prosiding FTSP Series.

Nasir, M. J., Iqbal, J., & Ahmad, W. (2020). Flash flood risk modeling of swat river sub-watershed: A comparative analysis of morphometric ranking approach and El-Shamy approach. *Arabian Journal of Geosciences*, *13*(20), 1082. https://doi.org/10.1007/s12517-020-06064-5

Nunn, P. D. (2009). *Vanished islands and hidden continents of the Pacific*. University of Hawai′i Press.

Obeidat, M., Awawdeh, M., & Al-Hantouli, F. (2021). Morphometric analysis and prioritisation of watersheds for flood risk

management in Wadi Easal Basin (WEB), Jordan, using geospatial technologies. *Journal of Flood Risk Management*, *14*(2), e12711. https://doi.org/10.1111/jfr3.12711

Ogden, F. L., Raj Pradhan, N., Downer, C. W., & Zahner, J. A. (2011). Relative importance of impervious area, drainage density, width function, and subsurface storm drainage on flood runoff from an urbanized catchment. *Water Resources Research*, *47*(12), 2011WR010550. https://doi.org/10.1029/2011WR010550

Padrón, R. S., Gudmundsson, L., Decharme, B., Ducharne, A., Lawrence, D. M., Mao, J., Peano, D., Krinner, G., Kim, H., & Seneviratne, S. I. (2020). Observed changes in dry-season water availability attributed to human-induced climate change. *Nature Geoscience*, *13*(7), 477–481. https://doi.org/10.1038/s41561-020-0594-1

Pownall, J. M., Hall, R., & Watkinson, I. M. (2013). Extreme extension across Seram and Ambon, eastern Indonesia: Evidence for Banda slab rollback. *Solid Earth*, *4*(2), 277–314. https://doi.org/10.5194/se-4-277-2013

Prasannakumar, V., Vijith, H., & Geetha, N. (2013). Terrain evaluation through the assessment of geomorphometric parameters using DEM and GIS: Case study of two major sub-watersheds in Attapady, South India. *Arabian Journal of Geosciences*, *6*(4), 1141–1151. https://doi.org/10.1007/s12517-011-0408-2

Rahmanda, A. S., & Dasanto, B. D. (2018). Penilaian Status Sumber Daya Air untuk Mitigasi Bencana Banjir dan Kekeringan: Studi Kasus Sub DAS Madiun: Assessment of Water Resource Status to Mitigate Flood and Drought Disasters: Case Study Madiun Sub Basin. *Jurnal Ilmu Tanah Dan Lingkungan*, *20*(2), 63–69. https://doi.org/10.29244/jitl.20.2.63-69

Rendra, P. P. R., & Sukiyah, E. (2021). Morphometric Characteristics of Cipeles Watershed to Identify Flood Prone Area. *International Journal on Advanced Science, Engineering and Information Technology*, *11*(3), 889–897. https://doi.org/10.18517/ijaseit.11.3.12937

Rendra, P. P. R. (2023). Quantitative Geomorphology Of Cipancar Watershed And The Implication For Flood Risk. *International Journal of GEOMATE*, *25*(111). https://doi.org/10.21660/2023.111.3573

Rudraiah, M., Govindaiah, S., & Vittala, S. S. (2008). Morphometry using remote sensing and GIS techniques in the sub-basins of Kagna river basin, Gulburga district, Karnataka, India. *Journal of the Indian Society of Remote Sensing*, *36*(4), 351–360. https://doi.org/10.1007/s12524-008-0035-x

Sambodo, T. H., Sukiyah, E., & Hutabarat, J. (2025). Stream Morphometry as Response to the Level of Tectonic Deformation on Sorowako and Surrounding Areas, Indonesia. *Journal of Geoscience, Engineering, Environment, and Technology*, *10*(3), 338–343. https://doi.org/10.25299/jgeet.2025.10.3.17977

Schumm, S. A. (1956). Evolution Of Drainage Systems And Slopes In Badlands At Perth Amboy, New Jersey. *Geological Society of America Bulletin*, *67*(5), 597. https://doi.org/10.1130/0016-7606(1956)67%255B597:EODSAS%255D2.0.CO;2

Şen, Z., Khiyami, H. A., Al-Harthy, S. G., Al-Ammawi, F. A., Al-Balkhi, A. B., Al-Zahrani, M. I., & Al-Hawsawy, H. M. (2013). Flash flood inundation map preparation for wadis in arid regions. *Arabian Journal of Geosciences*, *6*(9), 3563–3572. https://doi.org/10.1007/s12517-012-0614-6

Sinay, L. J., Lembang, F. K., Aulele, S. N., & Mustamu, D. (2020). Analisis Curah Hujan Bulanan Di Kota Ambon Menggunakan Model Heteroskedastisitas: Sarima-Garch. *Media Statistika*, *13*(1), 68–79. https://doi.org/10.14710/medstat.13.1.68-79

Soewarno. (1991). *Hidrologi: Pengukuran dan pengolahan data aliran sungai (hidrometri)*. Nova.

Spakman, W., & Hall, R. (2010). Surface deformation and slab–mantle interaction

during Banda arc subduction rollback. *Nature Geoscience*, *3*(8), 562–566. https://doi.org/10.1038/ngeo917

Sri Harto Br. (1993). *Analisis hidrologi*. Gramedia Pustaka Utama.

Srinivasa Vittala, S., Govindaiah, S., & Honne Gowda, H. (2004). Morphometric analysis of sub-watersheds in the Pavagada area of Tumkur district, South India, using remote sensing and GIS techniques. *Journal of the Indian Society of Remote Sensing*, *32*(4), 351–362. https://doi.org/10.1007/BF03030860

Strahler, A. N. (1957). Quantitative analysis of watershed geomorphology. *Eos, Transactions American Geophysical Union*, *38*(6), 913–920. https://doi.org/10.1029/TR038i006p00913

Strahler, A. (1964). Quantitative Geomorphology of Drainage Basins and Channel Networks. In *Handbook of Applied Hydrology*. (pp. 437–476). McGraw-Hill. https://www.scirp.org/reference/referencespapers?referenceid=1451624

Suhernomo, Fatah, L., Saidy, A. R., Priatmadi, B. J., Noor, I., & Triwibowo, D. (2023). Strategies of water flow treatment of Paringin Pit Lake to meet wastewater discharge compliance. *Journal of Degraded and Mining Lands Management*, *10*(4), 4683. https://doi.org/10.15243/jdmlm.2023.104.4683

Sukiyah, E., Sulaksana, N., Hendarmawan, H., & Rosana, M. F. (2009). Peran Morfotektonik DAS dalam Pengembangan Potensi Energi Mikro Hidro di Cianjur-Garut Bagian Selatan. *Bionatura*, *14*.

Sukiyah, E. (2012). The Morphometric Analysis on the Neotectonic Activities in Bandung Highland, West Java. *Majalah Geologi Indonesia*, *27*(3), 193–200.

Sukiyah, E., Syafri, I., Sjafrudin, A., Nurfadli, E., Khaerani, P., & Simanjuntak, D. (2015). Morphotectonic and satellite imagery analysis for identifying Quaternary fault at Southern part of Cianjur-Garut region, West Java, Indonesia. *The 36th Asian Conference on Remote Sensing*.

Sukiyah, E. (2017). *Sistem Informasi Geografis: Konsep dan Aplikasinya dalam Analisis Geomorfologi Kuantitatif.* Unpad Press.

Supartoyo, S., & Putranto, E. K. (2014). *Katalog Gempabumi Merusak di Indonesia Tahun 1612-2014*. Pusat Vulkanologi dan Mitigasi Bencana Geologi, Badan Geologi Bandung. https://anyflip.com/mcwnz/dijr

Sy, B., Frischknecht, C., Dao, H., Consuegra, D., & Giuliani, G. (2019). Flood hazard assessment and the role of citizen science. *Journal of Flood Risk Management*, *12*(S2), e12519. https://doi.org/10.1111/jfr3.12519

Terry, J. P., & Kostaschuk, R. (2007, July). *Merging concepts in hydrology in the South Pacific islands.* Asia Oceania Geosciences Society (AOGS), 4th Annual Conference, Bangkok, Thailand. https://www.researchgate.net/publication/332607533_Emerging_concepts_in_hydrology_in_the_South_Pacific_islands

Thornthwaite, C. W. (1948). An Approach toward a Rational Classification of Climate. *Geographical Review*, *38*(1), 55. https://doi.org/10.2307/210739

Tjokrosapoetro, S., Rusmana, E., & Achdan, A. (1993). *Peta Geologi Lembar Ambon, Maluku Skala 1:250.000* [Map]. Pusat Penelitian dan Pengembangan Geologi.

Triatmodjo, B. (2008). *Hidrologi Terapan* (Cetakan ke-7, 2019). Beta Offset.

Trifonova, T., Trifonov, D., & Arakelian, S. (2016). 2015 Disastrous Floods in Louisiana, USA, and Assam, India: Groundwater Impact on the Water Balance Estimation. *Hydrology*, *3*(4), 41. https://doi.org/10.3390/hydrology3040041

Tuanany, N. K., Sukiyah, E., Muslim, G. O., Muslim, D., Fikri, N. H., & Cahya, B. Y. (2024). Morphometric Characteristics of the Wairuhu River Watershed in Quaternary, Late Cenozoic, and Mesozoic Aged Rocks in the Framework of Encouraging Aspiring Geoparks in Ambon City, Maluku Province. *IOP Conference Series: Earth and Environmental Science*, *1424*(1), 012034. https://doi.org/10.1088/1755-1315/1424/1/012034

Tutuarima, C. T., Talakua, S. M., & Osok, R. M. (2021). Penilaian Degradasi Lahan dan Dampak Sedimentasi terhadap Perencanaan Bangungan Air di Daerah Aliran Sungai Wai Ruhu, Kota Ambon. *Jurnal Budidaya Pertanian*, *17*(1), 43–51. https://doi.org/10.30598/jbdp.2021.17.1.43

Usman, F., & Hamim, S. A. (2018). Determine Environmental Structure Condition of River Sub System of Palembang City's Rivers using Geospatial Analysis. *International Journal of Engineering & Technology*, *7*(4.35), 424. https://doi.org/10.14419/ijet.v7i4.35.22774

Van Zuidam, R. A. (1985). *Aerial Photo-Interpretation in Terrain Analysis and Geomorphology Mapping*. Smits Publishers.

Verstappen, H. T. (1983). *Applied Geomorphology: Geomorphological Surveys for Environmental Development*. International Institute for Aerial Survey and Earth Science (I.T.C).

Vinutha, D. N., & Janardhana, M. R. (2014). Morphometry of the Payaswini Watershed, Coorg District, Karnataka, India, Using Remote Sensing and GIS Techniques. *International Journal of Innovative Research in Science, Engineering and Technology (IJIRSET).*, *3*, 516–524.

Watkinson, I. M., Hall, R., Cottam, M. A., Sevastjanova, I., Suggate, S., Gunawan, I., Pownall, J. M., Hennig, J., Ferdian, F., Gold, D., Zimmermann, S., Rudyawan, A., & Advocaat, E. (2021). New Insights into the Geological Evolution of Eastern Indonesia from Recent Research Projects by the SE Asia Research Group. *Berita Sedimentologi*, *23*(1), 21–27. https://doi.org/10.51835/bsed.2012.23.1.189

Wattimena, L., & Handoko, W. (2016). Hunian Prasejarah di Jasirah Leihitu Pulau Ambon, Maluku. *Kapata Arkeologi*, *8*(2), 51. https://doi.org/10.24832/kapata.v8i2.186

Widyastuti, I., Mujiati, Dr., Jansen, D. I. R., & Yunus, A. F. (2024). Computational Simulation Of Sediment Motion Stability Process On Bridge Abutment Due To Crib Placement (Case Study: Harapan River, Jayapura Regency). *Rudarsko-Geološko-Naftni Zbornik*, *39*(4), 77–88. https://doi.org/10.17794/rgn.2024.4.6

Winarto, J., Sukiyah, E., Haryanto, A. D., & Haryanto, I. (2019). Morphotectonic study of a watershed controlled by active fault in Southern Garut, West Java, Indonesia. *Journal of Himalayan Earth Sciences*, *52*(2), 96–105.

Wohl, E. E. (2010). *Mountain rivers revisited*. American Geophysical Union/Geopress. https://doi.org/10.1029/WM019

Yuliana, S. (2008). *Kajian Ulang Hidrologi* [Tesis]. Universitas Indonesia.